CrystEngComm

Accepted Manuscript

ROYAL SOCIETY OF CHEMISTRY

www.rsc.org/crystengcomm

A Facile Strategy to Adjust the Density of Planar Triangle Units in Lead Borate-Nitrates

Jun-Ling Song, Xiang Xu, Chun-Li Hu, Fang Kong and Jiang-Gao Mao*

For Tables of Contents Only:

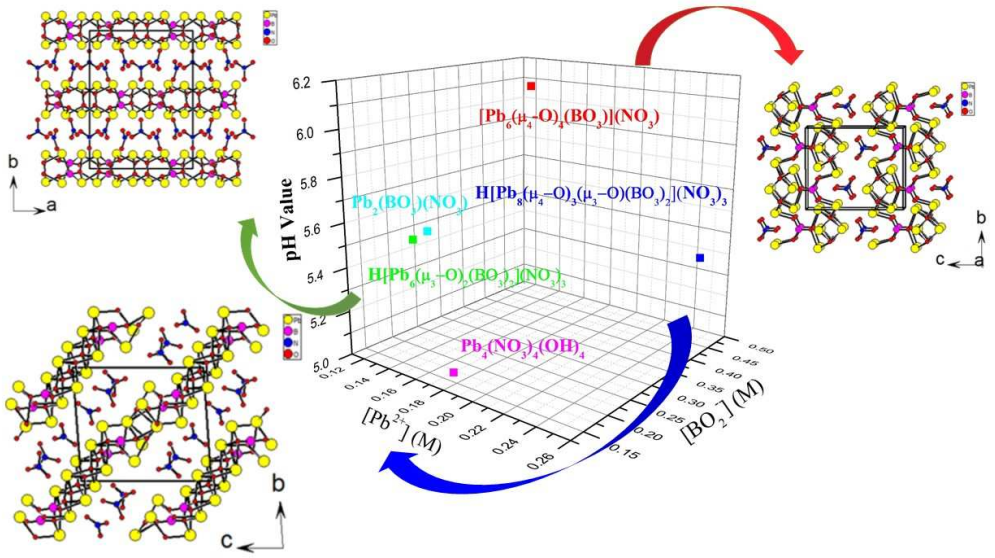

Three novel lead (II) borate-nitrates were obtained through a facile hydrothermal reaction by adjusting the concentrations of the starting materials.

Journal Name

RSCPublishing

ARTICLE

A Facile Strategy to Adjust the Density of Planar Triangle Units in Lead Borate-Nitrates

Cite this: DOI: 10.1039/xoxxoooooox

Jun-Ling Song, Xiang Xu, Chun-Li Hu, Fang Kong and Jiang-Gao Mao*

Received ooth January 2012,
Accepted ooth January 2012

DOI: 10.1039/xoxxoooooox

www.rsc.org/

Three novel lead (II) borate-nitrates were obtained through a facile hydrothermal reaction by adjusting the concentrations of the starting materials, namely, $[Pb_6(\mu_4\text{-}O)_4(BO_3)](NO_3)$ (**1**), $H[Pb_6(\mu_3\text{-}O)_2(BO_3)_2](NO_3)_3$ (**2**) and $H[Pb_8(\mu_4\text{-}O)_3(\mu_3\text{-}O)(BO_3)_2](NO_3)_3$ (**3**). All three compounds feature lead(II) oxo borate layers that are separated by nitrate anions. The 2D $[Pb_6(\mu_4\text{-}O)_4(BO_3)]^+$ layer parallel to the *ab* plane in **1** is built from 1D $[Pb_6(\mu_4\text{-}O)_4]^{4+}$ chains along the *a* axis and bridging borate anions. The 2D $H[Pb_6(\mu_3\text{-}O)_2(BO_3)_2]^{3+}$ layer in **2** which is perpendicular to the *b* axis is composed of "isolated" Pb^{2+} and tetranuclear $[Pb_4(\mu_3\text{-}O)_2]^{4+}$ clusters interconnected by bridging BO_3 groups. The $[Pb_8(\mu_4\text{-}O)_3(\mu_3\text{-}O)(BO_3)_2]^{2+}$ (011) layer in **3** is composed of two types of lead(II) oxo chains, namely, 1D chains of $[Pb_4(\mu_4\text{-}O)_2]^{4+}$ and 1D chains of $[Pb_4(\mu_4\text{-}O)(\mu_3\text{-}O)]^{4+}$, both elongated along the *a* axis, which are further interconnected by bridging borate anions. This study also demonstrates that a small change in the concentration of the starting materials could result in product with a different density of the π-conjugated planar units.

Introduction

Borate-based inorganic materials have become increasingly important and have been the focus of intensive investigations due to their important applications in opto-electronic technologies such as laser frequency conversion, optical parameter oscillator (OPO), and signal communication during the last few decades.[1-8] Borate crystals exhibit rich structural types, efficient frequency conversion capability, high UV transmittance to a wide range of wavelengths and high laser-damage threshold.[7-13] The rich structural chemistry for the metal borates can be attributed to presence of the trigonal planar BO_3 and tetrahedral BO_4 building units for the B element, and these two units can be interconnected via corner-sharing or edge-sharing to form various isolated B–O clusters as well as many extended B-O architectures.[14–20] In particular, borate materials containing the π-conjugated planar triangular BO_3 units that are properly aligned can show good NLO performance as exampled by KBe_2BO_3F (KBBF) and β-BaB_2O_4 (BBO) with $[BO_3]^{2-}$ and $[B_3O_6]^{3-}$ unit, respectivly.[7-8] According to the anionic group theory, the non-linear optical (NLO) properties of the materials could be significantly enhanced with the increase of the density of the planar conjugated π-conjugated groups.[21-24] Similar to the $[BO_3]^{3-}$ anion, other oxyanions such as carbonate[25-27] and nitrate groups[28-29] have been used as the building blocks to assemble materials with acentric structures and good NLO properties. Furthermore, lone pair containing cations such as Pb^{2+} have been combined with aboveπ-conjugated planar triangular units into a same compound and a few NLO materials based on lead(II) borates, carbonates or nitrates have been reported, among which $Pb_{16}(OH)_{16}(NO_3)_{16}$,[4c] $Pb_4O(BO_3)_2$ [4b] and $CsPbCO_3F$[26] showing large SHG responses of about 3.5，3.0, and 13.4 times that of KDP (KH_2PO_4), respectively. Recently we have been exploring metal mixed anion compounds containing two types of π-conjugated planar triangular units. We have isolated a series of lead-borates by only adjusting pH value using hydrothermal techniques,[29] two lead(II) borate-nitrate compounds, namely, centrosymmetric $Pb_3B_3O_7(NO_3)$[29a] and polar $Pb_2(BO_3)(NO_3)$ [29b]with second-harmonic generation (SHG) response of ~9.0 times that of KDP, were discovered. So far, metal borate-nitrates reported are still rare. In addition to the above two lead(II) nitrate-borates reported by our group, only two alkali metal borates-nitrates, namely, $Na_3(NO_3)(B_6O_{10})$[27a] and $K_3Na[B_6O_9(OH)_3]NO_3$, [27b] and three lanthanide or actinide borate-nitrates, namely, $Ce[B_5O_8(OH)]NO_3{\cdot}3H_2O$,[28a] $K_2[(NpO_2)_3B_{10}O_{16}(OH)_2(NO_3)_2]$[28b] and $La[B_5O_8(OH)]NO_3{\cdot}2H_2O$,[28c] have been reported. They display many structural types based on different polyborate anions. It is also shown that the polyborate anions exist in aqueous borate solutions depending on experimental conditions, such as, pH, reaction temperature, the concentration of boron and the counter-cation used.[29-35] We deem that the synthetic and structural chemistry for the metal borate-nitrate compounds require much more systematic investigation. As an extension of our previous works on lead(II) nitrate-borates, herein three new lead(II) borate-nitrates, namely, $[Pb_6(\mu_4\text{-}O)_4(BO_3)](NO_3)$ (**1**),

$H[Pb_6(\mu_3\text{-}O)_2(BO_3)_2](NO_3)_3$ (**2**) and $H[Pb_8(\mu_4\text{-}O)_3(\mu_3\text{-}O)(BO_3)_2](NO_3)_3$ (**3**), are reported.

Experimental section

Materials and instrumentation

$Pb(NO_3)_2$, PbO, $Mg(BO_2)_2\cdot H_2O$ and nitric acid solution (~35%) were analytically pure from Shanghai Reagent Factory (AR, 99.0%) and used without further purification.

IR spectra were recorded on a Magna 750 FT-IR spectrometer as KBr pellets in the range of 4000-450 cm^{-1}. Microprobe elemental analyses for the Pb, N and B elements were performed on a field-emission scanning electron microscope (FESEM, JSM6700F) equipped with an energy-dispersive X-ray spectroscope (EDS, Oxford INCA). Powder X-ray diffraction (XRD) patterns were collected on a Rigaku MiniFlex II diffractometer using Cu-Kα radiation with a step size of 0.02 °. Optical diffuse-reflectance spectra were measured at room temperature with a PE Lambda 900 UV-vis-NIR spectrophotometer. The $BaSO_4$ plate was used as a standard (100 % reflectance).[36] Thermogravimetric analysis (TGA) was carried out with a NETZSCH STA 449C unit at a heating rate of 15 °C/min under nitrogen atmosphere.

Syntheses

Crystals obtained in this study were grown by hydrothermal techniques. The mixture of $Pb(NO_3)_2$ or PbO, $Mg(BO_2)_2\cdot H_2O$ and H_2O were sealed in the autoclaves equipped with a Teflon liner (20 mL) and heated at 210 °C for 4 days. The amount of starting materials used are summarized in Table S1. The compounds were prepared by an analogous procedure. And the typical preparation processes of compound **1-3** is given.

Preparation of $[Pb_6(\mu_4\text{-}O)_4(BO_3)](NO_3)$ (1). PbO (0.5632 g), $Mg(BO_2)_2\cdot H_2O$ (0.1841 g) and HNO_3 (0.2 mL) were mixed in H_2O (12.0 mL) and sealed in an autoclave equipped with a Teflon liner (20 mL) and heated at 210 °C for 4 days. The initial and final pH values are 6.2 and 5.7, respectively. The colorless needle-like crystals of $[Pb_6(\mu_4\text{-}O)_4(BO_3)](NO_3)$ were obtained in a yield of ca. 80% based on Pb element. A number of experiments were tried to prepare a single phase of compound $[Pb_6(\mu_4\text{-}O)_4(BO_3)](NO_3)$ **(1)** using $Pb(NO_3)_2$ and $Mg(BO_2)_2\cdot H_2O$ as starting materials, such as changing the pH values, reaction times, and temperatures; however, only small amount of crystals were obtained. Finally, sufficient quantity of $[Pb_6(\mu_4\text{-}O)_4(BO_3)](NO_3)$ crystals was isolated in a yield of ca. 80% after sieving by ultrasound according to the above-mentioned process. Its purity was confirmed by a powder XRD study. The EDS analysis confirmed its Pb/N/B/O elemental composition. Its purity was confirmed by power XRD diffraction studies (Fig. S1a). IR data (KBr cm^{-1}): 1635 (w), 1389 (m), 1345 (s), 1254 (s), 1195 (m), 1163 (m), 817 (w), 729 (w), 706 (m), 638 (m), 567 (m), 470 (m), 419 (m).

Preparation of $H[Pb_6(\mu_3\text{-}O)_2(BO_3)_2](NO_3)_3$ (2). $Pb(NO_3)_2$ (0.5281 g) and $Mg(BO_2)_2\cdot H_2O$ (0.1502 g) were mixed in H_2O (12.0 mL) and sealed in an autoclave equipped with a Teflon liner (20 mL) and heated at 210 °C for 4 days. The initial and final pH values are 5.5 and 5.0, respectively. The colorless prism-like crystals of $H[Pb_6(\mu_3\text{-}O)_2(BO_3)_2](NO_3)_3$ (**2**) were obtained in a yield of ca. 70% based on Pb element. The presence of Pb/N/B/O elements in the **2** was confirmed by the EDS analysis. Its purity was confirmed by power XRD diffraction studies (Fig. S1b). IR data (KBr cm^{-1}): 3461 (w), 1639 (w), 1386 (s), 1354 (s), 1208 (s), 920 (m), 807 (w), 752 (w), 729 (m), 645 (m), 535 (w), 432 (m).

Preparation of $H[Pb_8(\mu_4\text{-}O)_3(\mu_3\text{-}O)(BO_3)_2](NO_3)_3$ (3). $Pb(NO_3)_2$ (0.4980 g) and $Mg(BO_2)_2\cdot H_2O$ (0.1760 g) were mixed in H_2O (6.0 mL) and sealed in an autoclave equipped with a Teflon liner (20 mL) and heated at 210 °C for 4 days. The initial and final pH values are 5.4 and 5.0, respectively. The colorless prism-shaped crystals of $H[Pb_8(\mu_4\text{-}O)_3(\mu_3\text{-}O)(BO_3)_2](NO_3)_3$ were obtained in a yield of ca. 75% based on Pb element. The EDS analysis confirmed the presence of Pb/N/B/O elements in **3**. Its purity was confirmed by power XRD diffraction studies (Fig. S1c). IR data (KBr cm^{-1}): 3566 (m), 3456 (m),1636 (w), 1487 (w), 1383 (s), 1198 (m), 1021(w), 981 (w), 921 (w), 833 (w), 704 (m), 612 (w), 561 (w), 541 (w), 5489 (w), 412 (m).

Table 1. Crystal data and structural refinements for $[Pb_6(\mu_4\text{-}O)_4(BO_3)](NO_3)$ (**1**), $H[Pb_6(\mu_3\text{-}O)_2(BO_3)_2](NO_3)_3$ (**2**) and $H[Pb_8(\mu_4\text{-}O)_3(\mu_3\text{-}O)(BO_3)_2](NO_3)_3$ (**3**).

Compound	**1**	**2**	**3**
Formula	$B_3N\ O_{10}Pb_6$	$HB_2N_3O_{17}Pb_6$	$HB_2N_3O_{19}Pb_8$
Fw	1427.96	1579.86	2026.18
Crystal system	orthorhombic	monoclinic	triclinic
Space group	*Pmmn*	*C*2/*c*	*P*-1
a/Å	5.7534(3)	12.589(7)	9.0637(3)
b/Å	9.4520(5)	15.197(7)	9.9713(4)
c/Å	11.2740(8)	9.669(5)	11.6123(5)
α(deg)	90.00	90.00	85.559(3)
β(deg)	90.00	115.502(8)	79.021(3)
γ(deg)	90.00	90.00	88.640(3)
V/Å3	613.09(6)	1669.6(15)	1027.14(7)
Z	2	4	2
D_c/g·cm^{-3}	7.735	6.285	6.551
μ(Mo K*α*)/mm^{-1}	82.125	60.380	65.403
GOF on F^2	1.086	0.979	0.924
R_1,wR_2 [$I>2\sigma(I)$]^a	0.0409, 0.0778	0.0472, 0.1116	0.0218, 0.0342
R_1, wR_2 (all data)	0.0511, 0.0817	0.0583, 0.1151	0.0268, 0.0364

$^a R_1 = \Sigma||F_o|-|F_c||/\Sigma|F_o|$, $\omega R_2 = \{\Sigma\omega[(F_o)^2\ (F_c)^2]^2/\Sigma\omega[(F_o)^2]^2\}^{1/2}$.

X-ray Crystallography

X-ray diffraction data collections for all three compounds were performed on an Agilent Technologies SuperNova Dual

Wavelength CCD diffractometer equipped with a graphite-monochromated Mo−Kα radiation (λ = 0.71073 Å) at 293 K. The data sets were corrected for Lorentz and polarization factors as well as absorption by the multi-scan method.[37a] All three structures were solved by direct methods and refined by full matrix least-squares fitting on F^2 using SHELX-97. [37b] All atoms were refined with anisotropic thermal parameters. For the sake of charge balance, protons in compounds **2** and **3** were needed but they were not refined due to the difficulty in the determination of their precise locations.[38] The disorder of oxygen atom O(14) from non-coordination NO_3^- anions in compound **3** results in a big thermal ellipsoid of O(14) atom, which could be a split situation as reported by Henry el al.[39] The structures were also checked for possible missing symmetry with PLATON and none was found.[37c] Crystallographic data and structural refinements for the three compounds are summarized in Table 1. Important bond distances are listed in Table 2. More information of the crystallographic studies are given as Supporting Information Table S2-4. Further details of the crystal structure studies can be obtained from the FIZ Karlsruhe, 76344 Eggenstein-Leopoldshafen, Germany (Fax: (49)7247808666; E-mail: crysdata@fiz-karlsruhe.de), on quoting the depository numbers CSD 429078, 429079 and 429080.

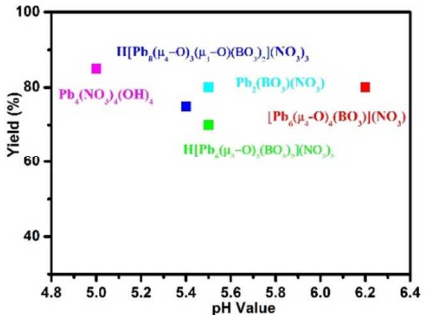

Chart 1. Products obtained at different pH value.

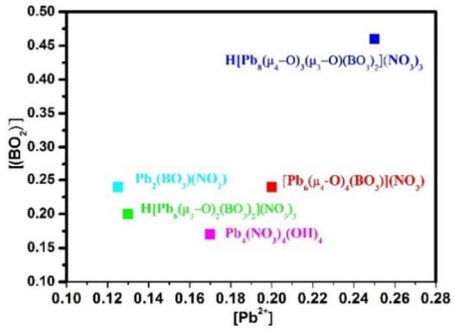

Chart 2. Products obtained at different concentration of starting materials.

Results and discussion

Our systematic explorations in the lead(II)-BO_3-NO_3 system resulted in the isolation of five different complexes, namely, $[Pb_6(\mu_4\text{-}O)_4(BO_3)](NO_3)$ (**1**), $H[Pb_6(\mu_3\text{-}O)_2(BO_3)_2](NO_3)_3$ (**2**) and $H[Pb_8(\mu_4\text{-}O)_3(\mu_3\text{-}O)(BO_3)_2](NO_3)_3$ (**3**), in addition to $Pb_2(BO_3)(NO_3)$[29b] and $Pb_4(NO_3)_4(OH)_4$[40b] reported previously. The products obtained in different concentration of starting material and different initial pH values are presented in Chart 1-2 and Chart S1-2. Combined with the synthesis conditions, the amount of the starting materials leads to the different pH value of the reaction system as shown in Chart S1. Thus, in this study, we mainly discuss the relationship between the concentration of starting materials and the final products. When the concentrations of $Pb(NO_3)_2$ and $Mg(BO_2)_2{\cdot}H_2O$ are 0.21 M and 0.12 M, respectively, needle-like crystals of $[Pb_6(\mu_4\text{-}O)_4(BO_3)](NO_3)$ (**1**) were obtained; changing the concentrations of $Pb(NO_3)_2$ and $Mg(BO_2)_2{\cdot}H_2O$ to 0.13 M and 0.10 M, respectively, afforded colourless prism-like crystals of $H[Pb_6(\mu_3\text{-}O)_2(BO_3)_2](NO_3)_3$ (**2**); With the increasing of the concentrations of $Pb(NO_3)_2$ and $Mg(BO_2)_2{\cdot}H_2O$ to 0.25 M and 0.23 M, respectively, colourless prism-like crystals of $H[Pb_8(\mu_4\text{-}O)_3(\mu_3\text{-}O)(BO_3)_2](NO_3)_3$ (**3**) were obtained; when the concentrations of $Pb(NO_3)_2$ and $Mg(BO_2)_2{\cdot}H_2O$ are 0.13 M and 0.12 M, respectively, large lamellar crystals of $Pb_2(BO_3)(NO_3)$[29b] were isolated; $Pb_4(NO_3)_4(OH)_4$ were obtained under concentrations of $Pb(NO_3)_2$ and $Mg(BO_2)_2{\cdot}H_2O$, to be 0.17M and 0.08M. Results of this work show that the concentrations of starting materials plays a very important role on the adjustment of the density of planar triangle units in lead borate-nitrates systems.

Crystal structure of $[Pb_6(\mu_4\text{-}O)_4(BO_3)](NO_3)$ (1). The structure of $[Pb_6(\mu_4\text{-}O)_4(BO_3)](NO_3)$ **(1)** features 2D lead(II) oxo borate layers that are separated by nitrate groups (Fig. 1). The asymmetric unit of **1** includes four Pb, one B, one N and five O atoms, totally eleven crystallographically independent atoms. Both Pb(1) and Pb(3) are three-coordinated whereas Pb(2) and Pb(4) atoms are four coordinated, their coordination geometries can be described as Ψ-PbO_3 trigonal pyramid and Ψ-PbO_4 tetragonal pyramid, respectively, where Ψ represents the lone pair electrons of the lead(II) cation. The Pb-O distances range from 2.24(2) Å to 2.379(9) Å. The oxo anion (O(5)) connects with four lead(II) cations to form an OPb_4 tetrahedron. The interconnection of lead(II) ions by oxo anions resulted in a 1D lead oxide slab along the *a* axis (Fig. 1a). These lead(II) oxide slabs are further bridged by borate anions into a 2D lead(II) oxo borate layer perpendicular to the *c* axis (Fig. 1b). Each BO_3 triangle connects with four lead(II) cations from three lead(II) oxide slabs. The nitrate anions remain non-coordinated and are located at interlayer space (Fig. 1c), which is similar to those reported in metal nitrate-borates.[24,29] B atom is in a BO_3 triangular coordination geometry, and the B−O bonds and O−B−O bond angles for the BO_3 unit are in the range of 1.36(5)−1.38(3) Å and 118.1(18)−124(4)°, respectively. In contrast, the N−O bonds and O−N−O bond angles for the NO_3 unit range from 1.19(3)−1.27(5) Å and 119(3)−122(5)°, respectively (Table 2). These bond distances and angles are close to those reported in other borates.[4, 22, 29] The $B(1)O_3$ and $N(1)O_3$ triangles adopt a layered-type arrangement and are aligned in a perfect parallel fashion in the

(100) plane with a dihedral angle of 0.0° between the two triangular planes. The calculated total bond valences for Pb(1), Pb(2), Pb(3), and Pb(4) are 2.09, 2.16, 1.92, and 2.08, respectively, and those for B and N are 2.98 and 5.39, respectively, indicating that Pb, B and N atoms are in oxidation states of +2, +3, and +5, respectively.[29,40]

Table 2. Selected bond distances (Å) for compounds **1**-**3**[a].

$[Pb_6(\mu_4\text{-}O)_4(BO_3)](NO_3)$ (**1**)			
Pb(1)-O(2)#1	2.24(2)	Pb(1)-O(5)	2.248(10)
Pb(1)-O(5)#2	2.248(10)	Pb(2)-O(5)#3	2.340(10)
Pb(2)-O(5)	2.340(10)	Pb(2)-O(5)#2	2.340(10)
Pb(2)-O(5)#4	2.340(10)	Pb(3)-O(5)#6	2.235(10)
Pb(3)-O(5)	2.235(10)	Pb(3)-O(1)	2.379(9)
Pb(4)-O(5)	2.353(10)	Pb(4)-O(5)#3	2.353(10)
Pb(4)-O(5)#5	2.353(10)	Pb(4)-O(5)#6	2.353(10)
B(1)-O(2)	1.38(3)	B(1)-O(2)#5	1.38(3)
B(1)-O(1)	1.36(5)	N(1)-O(4)	1.19(3)
N(1)-O(4)#7	1.19(3)	N(1)-O(3)	1.27(5)
$H[Pb_6(\mu_3\text{-}O)_2(BO_3)_2](NO_3)_3$ (**2**)			
Pb(1)-O(2)#1	2.318(10)	Pb(1)-O(1)#2	2.328(11)
Pb(1)-O(2)	2.330(10)	Pb(2)-O(9)	2.253(10)
Pb(2)-O(3)	2.279(10)	Pb(2)-O(1)#2	2.376(10)
Pb(3)-O(3)#2	2.255(10)	Pb(3)-O(9)	2.339(10)
Pb(3)-O(9)#3	2.379(9)	B(1)-O(2)	1.352(16)
B(1)-O(1)	1.361(15)	B(1)-O(3)	1.419(17)
N(1)-O(5)	1.217(19)	N(1)-O(6)	1.256(17)
N(1)-O(4)	1.298(16)	N(2)-O(7)	1.245(18)
N(2)-O(8)	1.247(13)	N(2)-O(8)#4	1.247(13)
$H[Pb_8(\mu_4\text{-}O)_3(\mu_3\text{-}O)(BO_3)_2](NO_3)_3$ (**3**)			
Pb(1)-O(19)#1	2.354(6)	Pb(1)-O(18)	2.373(5)
Pb(1)-O(19)	2.381(5)	Pb(1)-O(3)	2.602(6)
Pb(2)-O(19)	2.226(6)	Pb(2)-O(5)	2.330(6)
Pb(2)-O(3)	2.399(5)	Pb(2)-O(6)	2.628(6)
Pb(3)-O(18)	2.202(6)	Pb(3)-O(19)#1	2.348(6)
Pb(3)-O(6)#1	2.569(6)	Pb(3)-O(2)#2	2.636(5)
Pb(4)-O(17)	2.227(6)	Pb(4)-O(6)#3	2.269(5)
Pb(4)-O(2)#4	2.393(6)	Pb(5)-O(18)	2.332(5)
Pb(5)-O(18)#2	2.333(5)	Pb(5)-O(2)	2.405(6)
Pb(5)-O(3)	2.516(6)	Pb(6)-O(17)	2.250(6)
Pb(6)-O(17)#4	2.279(6)	Pb(6)-O(4)#3	2.305(5)
Pb(7)-O(4)#3	2.363(6)	Pb(7)-O(16)	2.425(6)
Pb(7)-O(16)#3	2.567(5)	Pb(7)-O(17)#4	2.573(5)
Pb(7)-O(1)	2.749(6)	Pb(8)-O(1)	2.175(6)
Pb(8)-O(16)	2.255(6)	Pb(8)-O(5)	2.292(5)
B(1)-O(1)	1.334(12)	B(1)-O(2)	1.396(11)
B(1)-O(3)	1.435(11)	B(2)-O(4)	1.361(12)
B(2)-O(6)	1.358(11)	B(2)-O(5)	1.400(11)
N(1)-O(9)	1.204(9)	N(1)-O(7)	1.249(10)
N(1)-O(8)	1.274(9)	N(2)-O(10)	1.251(10)
N(2)-O(12)	1.255(11)	N(2)-O(11)	1.276(9)
N(3)-O(14)	1.208(13)	N(3)-O(15)	1.220(11)
N(3)-O(13)	1.228(10)		

[a] Symmetry transformations used to generate equivalent atoms: for **1**: #1 -x, -y, -z; #2 -x-1/2, y, z; #3 x, -y+1/2, z; #4 -x-1/2, -y+1/2, z; #5 -x+1/2, -y+1/2, z; #6 -x+1/2, y, z; #7 -x+1/2, -y+3/2, z; for **2**: #1 -x, -y, -z; #2 x, -y, z-1/2; #3 -x+1, -y, -z; #4 -x+1, y, -z+1/2; #5 x, -y, z+1/2; for **3**: #1 -x, -y, -z; #2 -x+1, -y, -z; #3 -x, -y-1, -z+1; #4 -x+1, -y-1, -z+1.

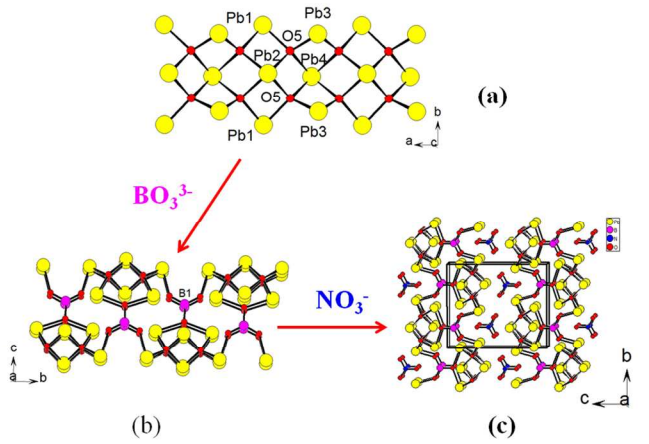

Fig. 1 A lead(II) oxo chain along the *a*-axis (a), a lead(II) oxo borate layer perpendicular to the *c* axis (b), and view of structure of compound **1** down the *a* axis (c).

Crystal structure of $H[Pb_6(\mu_3\text{-}O)_2(BO_3)_2](NO_3)_3$ (2). The structure of compound **2** features a different lead(II) oxo borate layer normal to the *b* axis, these 2D layers are separated by non-coordination nitrate groups as in compound **1** (Fig. 2). The asymmetric unit of **2** contains fifteen unique non-H atoms, including three Pb, one B, two N and nine O atoms. Pb(1) is three coordinated by three borate oxygens whereas Pb(2) and Pb(3) are three coordinated by one oxo anion (O9) and two oxygens from two borate groups. The Pb-O distances are in the range of 2.253(10)–2.379(9) Å. The coordination geometries around these lead(II) can be described as a Ψ-PbO_3 trigonal pyramid where Ψ represents the lone pair electrons of the lead(II) cation as in **1**. The oxo anion acts as a μ_3 bridging ligand which connects with one Pb(2) and two Pb(3) atoms. Pb(2) and Pb(3) atoms form a $Pb_4(\mu_3\text{-}O)_2$ tetranuclear cluster. These $Pb_4(\mu_3\text{-}O)_2$ tetranuclear clusters and "isolated" Pb(1) atoms are bridged by borate anions into a lead(II) oxo borate layer parallel to the *ac* plane (Fig. 2a). The interlayer distance is approximately 7.6 Å (half of the *b* axis). Each borate group connects with six lead(II) ions and all three oxygen atoms are bidentately bridging. The B–O bond lengths and O–B–O bond angles range from 1.352(16) to 1.419(17) Å and 114.4(12) to 129.0(14) °, respectively. The nitrate groups act as interlayer spacers (Fig. 2b), and the N–O bond lengths and O–N–O bond angles range from 1.217(19) to 1.298(16) Å and 116.1(14) to 122.2(17) °, respectively. The calculated total bond valances for Pb(1), Pb(2), Pb(3), B(1), N(1) and N(2) is 1.69, 1.81, 1.71, 2.96, 4.83 and 4.96, respectively, indicating that Pb, B and N atoms are in oxidation states of +2, +3, and +5, respectively.[38] The deviation of the Pb atoms from the expected Bond Valence Sum (BVS) values of +2 indicate that there are other weak Pb-O bonds (Pb-O 2.8-3.3 Å).

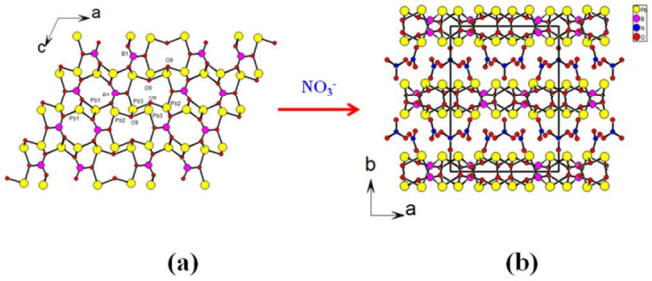

Fig. 2 A lead(II) oxo borate layer perpendicular to the *b* axis (a) and view of crystal structure of compound **2** down the *c* axis (b).

Different from those in **1**, the nitrate groups and borate groups are not arranged in a parallel fashion. The dihedral angle between $N(1)O_3$ and $N(2)O_3$ groups is 80.8 ° and those between $B(1)O_3$ and the two nitrate groups are 64.8 and 89.3 °, hence these two triangular units are more close to perpendicular to each other.

Crystal structure of $H[Pb_8(\mu_4\text{-}O)_3(\mu_3\text{-}O)(BO_3)_2](NO_3)_3$ (3). The structure of compound **3** features a different lead(II) oxo borate layer from those of **1** and **2** (Fig. 3). The (011) lead(II) oxo borate layer is composed of two different lead(II) oxide chains, namely, 1D chains of $[Pb_4(\mu_4\text{-}O)_2]^{4+}$ and 1D chains of $[Pb_4(\mu_4\text{-}O)(\mu_3\text{-}O)]^{4+}$, both elongated along the *a* axis, which are interconnected by bridging borate groups. Neighboring lead(II) oxo borate layers are separated by non-coordination nitrate anions (Fig. 3). The asymmetric unit of **2** contains thirty-two crystallographically independent non-H atoms, including eight Pb, three N, two B and nineteen O atoms. The eight Pb atoms possess different coordination environments. Among eight Pb atoms, Pb(4), Pb(6) and Pb(8) are three coordinated, Pb(1), Pb(2), Pb(3) and Pb(5) are 4-coordinated whereas Pb(7) is five coordinated. They coordination geometries can be described as Ψ-PbO_3 trigonal pyramid, Ψ-PbO_4 tetragonal pyramid and Ψ-PbO_5 octahedron, respectively, where Ψ represents the lone pair electrons of the lead(II) cation. The Pb-O distances are in the range of 2.202(6) to 2.749(6) Å. Among four oxide anions, O(16) is tridentate metal linker whereas O(17), O(18) and O(19) are tetradentate metal linkers. Pb(1), Pb(2), Pb(3) and Pb(5) are interconnected by O(18) and O(19) atoms into a 1D chain of $[Pb_4(\mu_4\text{-}O)_2]^{4+}$ along the *a* axis (Fig. 3a) whereas Pb(4), Pb(6), Pb(7) and Pb(8) atoms bond with O(16) and O(17) atoms to form a 1D chain of $[Pb_4(\mu_4\text{-}O)(\mu_3\text{-}O)]^{4+}$ also along the *a* axis (Fig. 3b). The above two types of lead oxide chains are bridged by borate anions into a (011) lead oxo borate layer (Fig. 3c). The $B(1)O_3$ group bonds with seven lead(II) cations, two oxygen atoms are tridentate whereas the third one is bidentate, differently, the $B(2)O_3$ group connects with six lead(II) cations, two oxygen atoms are bidentate whereas the third one is tridentate. The B-O distances fall in the range of 1.334(12) to 1.435(11) Å, and the O-B-O bond angles range from 114.5(9) to 125.4(8) °. The nitrate anions act as interlayer spacers as in **1** and **2** (Fig. 3d), the N-O and O-N-O bond distances and angles are in the range of 1.204(9)-1.276(9) Å and 117.5(10)-

122.2(10)°, respectively(Table S4). The calculated total bond valences for Pb(1) to Pb(8) are 1.76, 2.00, 1.85, 1.85, 1.89, 1.92, 1.69 and 2.13, respectively, and those for B(1), B(2), N(1), N(2) and N(3) are 2.88, 2.99, 5.02, 4.77 and 5.34, respectively, indicating that Pb, B and N atoms are in oxidation states of +2, +3, and +5, respectively.[38] The deviation of some Pb atoms from the expected BVS values of +2 indicate that there are weak Pb-O bonds (Pb-O 2.8-3.3 Å).

The borate groups and nitrate groups in **3** are not aligned in a parallel fashion as in **2**. The dihedral angle between $B(1)O_3$ and $B(2)O_3$ groups is 26.1°, whereas the dihedral angles between the nitrate groups are in the range of 20.6 -78.6°. The dihedral angles between the nitrate and borate groups are in the range of 62.8 -130.0°.

It is interesting to compare the densities of the planar triangular groups in above compounds and $Pb_2(BO_3)(NO_3)$ we reported recently.[29b] They are 0.00652, 0.0120, 0.00974 and 0.0138/Å^3, respectively for compounds **1**, **2**, **3** and $Pb_2(BO_3)(NO_3)$. Hence the polar $Pb_2(BO_3)(NO_3)$ has the highest density of the triangular groups and in the meantime all of these structure units are aligned perfectly to produce a very large SHG response.[29b]

Optical Properties.

The optical properties of these three new compounds were examined by diffuse-reflectance spectra at room temperature. It is clear that these compounds show a strong absorption in the region of 200 to 378 nm, 200 to 328 and 200 to 324 nm, respectively for compounds **1-3** (Fig. S2). All of them show little absorption in the range of 410-2500 nm. Hence, these compounds are almost transparent in the range of 0.40−2.50 μm. These three compounds are wide band-gap semiconductors with optical band gaps of 3.27, 3.66, and 4.09 eV, respectively

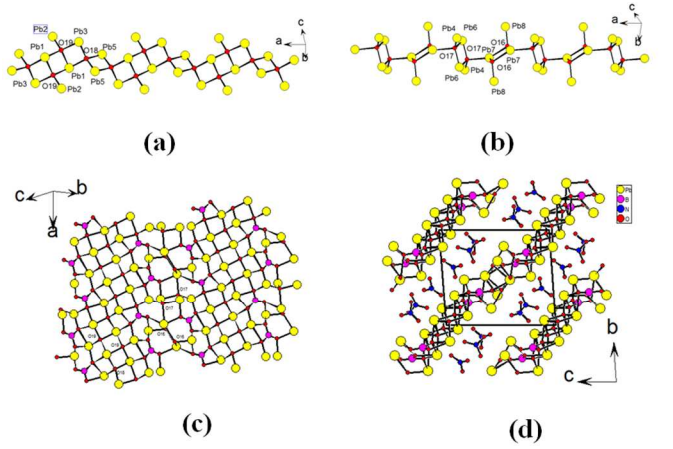

Fig. 3 A lead(II) oxo chain along the *a*-axis formed by Pb(1), Pb(2), Pb(3) and Pb(5) (a), A lead(II) oxo chain along the *a*-axis formed by Pb(4), Pb(6), Pb(7) and Pb(8) (b), a (011) lead(II) oxo borate layer (c), and view of crystal structure of compound **3** down the *a* axis (d).

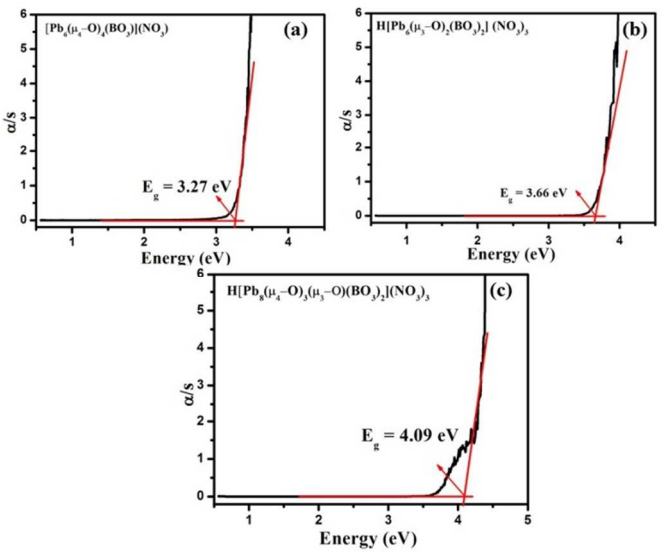

Fig. 4 UV-Vis-NIR absorption spectra for $[Pb_6(\mu_4\text{-}O)_4(BO_3)](NO_3)$ (**a**), $H[Pb_6(\mu_3\text{-}O)_2(BO_3)_2](NO_3)_3$ (**b**) and $H[Pb_8(\mu_4\text{-}O)_3(\mu_3\text{-}O)(BO_3)_2](NO_3)_3$ (**c**).

for compounds **1-3** (Fig. 4). IR spectra of these compounds showed strong absorption peaks at around 1380 cm^{-1} which confirms the presence of NO_3^- group, whereas the absorption peaks in the frequency range 1350–1100 cm^{-1} can be attributed to the asymmetric stretch (ν_{as}), bands from 1000-800 cm^{-1} associated with symmetric stretch (ν_s) of BO_3 groups, absorption bands from 780 to 600 cm^{-1} due to out-of-plane bending vibrations (γ) of BO_3 groups , and bands from 590 to 500 cm^{-1} may be assigned as the BO_3 in-plane bending modes (δ). Hence the IR data confirms the presence of BO_3 triangular and absence of BO_4 tetrahedron in all three compounds, which is in good agreement with the results obtained from the single-crystal X-ray structural analyses (Fig. S3).[40-41]

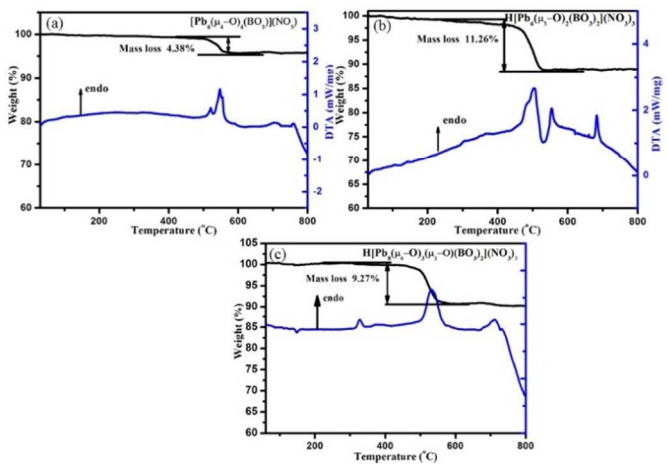

Fig. 5 TGA and DSC curves for $[Pb_6(\mu_4\text{-}O)_4(BO_3)](NO_3)$ (**a**), $H[Pb_6(\mu_3\text{-}O)_2(BO_3)_2](NO_3)_3$ (**b**) and $H[Pb_8(\mu_4\text{-}O)_3(\mu_3\text{-}O)(BO_3)_2](NO_3)_3$ (**c**).

TGA Studies.

Thermogravimetric analysis (TGA) of the three compounds show similar decomposition process under nitrogen atmosphere

(Fig. 5). Compound **1** is stable up to about 467 °C and displays one step of weight loss, the weight loss in the in the temperature range of 467−570 °C, corresponding to the decomposition of the NO_3 groups, which is in agreement with the one apparent endothermic peaks observed at 547 ^oC in the thermal analysis (DTA) diagram. Compound **2** is thermally stable up to about 330 °C and the weight loss in the temperature range 330-578 ^oC corresponds to the release of H_2O and decomposition of the nitrate anions, which is in agreement with the two apparent endothermic peaks observed at 326 °C and 535 ^oC, respectively, in the thermal analysis (DTA) diagram. Compound **3** shows a weight loss of about 11.26% in the range from 290 to 530 °C, which may be associated with the release of the nitrate groups and the water molecules and two distinct endothermic peaks in this temperature range can be found in the DTA curves. The final residuals of the three compounds are not characterized because of their amorphous nature.

Conclusions

In summary, by only adjusting the concentrations of the starting materials, a series of different lead (II) compounds containing planar anionic units of BO_3 and NO_3 were obtained in high yields via a facile hydrothermal reaction, namely, $[Pb_6(\mu_4\text{-}O)_4(BO_3)](NO_3)$ (**1**), $H[Pb_6(\mu_3\text{-}O)_2(BO_3)_2](NO_3)_3$ (**2**) and $H[Pb_8(\mu_4\text{-}O)_3(\mu_3\text{-}O)(BO_3)_2](NO_3)_3$ (**3**). All three compounds feature lead(II) oxo borate layers that are separated by nitrate anions. Further these compounds show different lead(II) oxo clusters or 1D chains. This study demonstrates that a small change in the concentration of the starting materials could result in product with a different density of the π-conjugated planar units. We believe that the same synthetic method may be applied to other related systems such as bismuth(III) oxo nitrate borates and studies on these systems are underway in our laboratory.

Acknowledgements

This work was supported by the National Natural Science Foundation of China (Nos. 2123006, 21403232 and 2137222).

Notes and references

State Key Laboratory of Structural Chemistry, Fujian Institute of Research on the Structure of Matter, Chinese Academy of Sciences, Fuzhou 350002, People's Republic of China. E-mail: mjg@fjirsm.ac.cn; Tel: +86 591-83794836.

†Electronic Supplementary Information (ESI) available: X-ray crystallographic files in CIF format, simulated and experimental powder XRD patterns, IR, UV absorption spectra. CSD numbers 429078-429080. See DOI: 10.1039/b000000x/

1 K. M. Ok, E. O. Chi and P. S. Halasyamani, *Chem. Soc. Rev.*, 2006, **35**, 710-717.

2 S. V. Krivovichev, O. Mentré, O. I. Siidra, M. Colmont and S. K. Filatov, *Chem. Rev.*, 2013, **113**, 6459−6535.

3 R. Mu, Q. Fu, L. Jin, L. Yu, G. Fang, D. Tan and X. Bao, *Angew. Chem., Int. Ed.,* 2012, **51**, 4856−4859.

4 (a) H. Wu, S. Pan, K. R. Poeppelmeier and J. M. Rondinelli, *J. Am. Chem. Soc.*, 2013, **135**, 4215-4218; (b) H. W. Yu, S. L. Pan, H. P. Wu, W. W. Zhao, F. F. Zhang, H. Y. Li and Z. H. Yang, *J. Mater. Chem.*, 2012, **22**, 2105-2110; (c) L. X. Chang, L. Wang, X. Su, S. L. Pan, R. Hailili, H.W. Yu and Z. H. Yang, *Inorg. Chem.*, 2014, **53**, 3320-3325.

5 H. Huang, J. Yao, Z. Lin, X. Wang, R. He, W. Yao, N. Zhai and C. Chen, *Angew. Chem., Int. Ed.* 2011, **50**, 9141-9144.

6 C. T. Chen, Y. B. Wang, B. C. Wu, K. C. Wu, W. L. Zeng and L. H. Yu, *Nature*, 1995, **373**, 322-324.

7 (a) C. T. Chen and G. Z. Liu, *Annu. Rev. Mater. Res*,. 1986, **16**, 203-243; (b) C. T. Chen, B. C. Wu, A. D. Jiang and G. M. You, *Sci. Sin. B*, 1985, **28**, 235-241.

8 (a) C. T. Chen, Y. C. Wu, A. D. Jiang, B. C. Wu, G. M. You, R. K. Li and S. J. Lin, *J. Opt. Soc. Am. B*, 1989, **6**, 616-621; (b) Z. Lin, J. Lin, Z. Wang, C. T. Chen and M. H. Lee, *Phys. Rev. B*, 2000, **62**, 1757−1764.

9 Z.-T. Yu, Z. Shi, Y.-S. Jiang, H.-M. Yuan and J.-S. Chen, *Chem. Mater.*, 2002, **14**, 1314-1318.

10 J. Lin and M. Lee, *Phys. Rev. B* 1999, **60**, 13380-13389.

11 Z. Lin, J. Lin, Z. Wang, C. T. Chen and M. H. Lee, *Phys. Rev. B*, 2000, **62**, 1757-1764.

12 F. Pan, G. Shen, R. Wang, X. Wang and D. Shen, *J. Cryst. Growth* 2002, **241**, 108-114.

13 F. C. Hawthorne, P. C. Burns and J. D. Grice, *Crystal chemistry of boron, Reviews in Mineralogy: Boron Mineralogy, Petrology and Geochemistry*, Mineralogical Society of America, Washington, D. C., 2002, **33**, 41–116.

14 D. M. Schubert, M. Z. Visi, and C. B. Knobler, *Inorg. Chem.*, 2008, **47**, 2017-2023.

15 M. A. Beckett, P. N. Horton, S. J. Coles and D. W. Martin, *Inorg. Chem.*, 2011, **50**, 12215-12218.

16 D. M. Schubert, M. Z. Visi, S. Khan and C. B. Knobler, *Inorg. Chem.*, 2008, **47**, 4740-4745.

17 M. Z. Visi, C. B. Knobler, J. J. Owen, M. I. Khan and D. M. Schubert, *Cryst. Growth Des.*, 2006, **6**, 538-545.

18 L.-Z. Wu, L. Cheng, J.-N. Shen, and G.-Y. Yang, *CrystEngComm.*, 2013, **15**, 4483-4488.

19 S. Merlino, and F. Sartori, *Science*, 1971, **171**, 377-379.

20 W. J. Yao, X. X. Jiang, H. W. Huang, T. Xu, X. S. Wang, Z. S. Lin and C. T. Chen, *Inorg. Chem.*, 2013, **52**, 8291-8293.

21 L. Cheng, Q. Wei, H. Q. Wu, L.-J. Zhou and G.-Y. Yang, *Chem. Eur. J.,* 2013, **19**, 17662-17667.

22 H.-R. Tian, W.-H. Wang, Y.-E. Gao, T.-T. Deng, J.-Y. Wang, Y.-L. Feng and J.-W. Cheng, *Inorg. Chem.*, 2013, **52**, 6242-6244.

23 L. Wu, X. L. Chen, Y. P. Xu and Y. P. Sun, *Inorg. Chem.*, 2006, **45**, 3042-3047.

24 L. Y. Li, G. B. Li, Y. X. Wang, F. H. Liao and J. H. Lin, *Chem. Mater.*, 2005, **17**, 4174-4180.

25 J. Zhao and R. K. Li, *Inorg. Chem.*, 2012, **51**, 4568-4571.

26 G. H. Zou, L. Huang, N. Ye, C. S. Lin, W. D. Cheng and H. Huang, *J. Am. Chem. Soc.*, 2013, **135**, 18560–18566.

27 a) O. V. Yakubovich, I. V. Perevoznikova, O. V. Dimitrova and V. S. Urusov, *Dokl. Phys.*, 2002, **47**, 791-797; b) T. S. Ortner, K. Wurst, L. Perfler, M. Tribus and H. Huppertz, *J. Solid State Chem.*, 2015, **221**, 66-72.

28 a) L. Y. Li, X. L. Jin, G. B. Li, Y. X. Wang, F. H. Liao, G. Q. Yao and J. H. Lin, *Chem. Mater.*, 2003, **15**, 2253-2260; b) S. Wang, E. V. Alekseev, W. Depmeier and T. E. Albrecht-Schmitt, *Chem. Commun.*, 2010, **46**, 3955-3957; c) B.-C. Zhao, W. Sun, W.-J. Ren, Y.-X. Huang, Z. Li, Y. Pan and J.-X. Mi, *J. Solid State Chem.*, 2013, **206**, 91-98.

29 (a) J.-L. Song, C.-L. Hu, X. Xu. F. Kong and Mao, J.-G. *Inorg. Chem.*, 2013, **52**, 8979-8986; (b) J.-L. Song, C.-L. Hu, X. Xu, F. Kong and J.-G. Mao, *Angew. Chem., Int. Ed.,* 2015, **54**, 3679-3682.

30 M. J. Polinski, S. Wang, E. V. Alekseev, J. N. Cross, W. Depmeier and T. E. Albrecht-Schmitt, *Inorg. Chem.*, 2012, **51**, 11541-11548.

31 S. Wang, E. M. Villa, J. Diwu, E. V. Alekseev, W. Depmeier and T. E. Albrecht-Schmitt, *Inorg. Chem.*, 2011, **50**, 2527-2533.

32 I. D. Williams, M. M. Wu, H. H-Y. Sung, X. X. Zhang, J. H. Yu, *Chem. Commun.*, 1998, 2463-2464.

33 C. F. Sun, C. L. Hu, X. Xu, F. Kong and J. G. Mao, *J. Am. Chem. Soc.*, 2011, **133**, 5561-5573.

34 K. Ishihara, K. Nagasawa, K. Umemoto, H. Ito and K. Saito, *Inorg. Chem.*, 1994, **33**, 3811-3816.

35 Flanagan, J.; Griffith, W. P.; Powell, R. D. and West, A. P. *J. Chem. Soc. Dalton Trans.,* 1989, 1651-1655.

36 W. M. Wendlandt and H. G. Hecht, *Reflectance Spectroscopy*; Interscience: New York, 1966.

37 (a) *CrystalClear*, Version 1.3.5; Rigaku Corp.: Woodlands, TX, 1999. (b) G. M. Sheldrick, *SHELXTL*, Crystallographic Software Package, SHELXTL, Version 5.1; Bruker-AXS: Madison, WI, 1998. (c) A. L. Spek, *J. Appl. Crystallogr.*, 2003, **36**, 7-13.

38 (a) I. D. Brown and D. Altermatt, *Acta Crystallogr. B* 1985, **41**, 244-247; (b) N. E. Brese and M. O'Keeffe, *Acta Crystallogr. B* 1991, **47**, 192-197.

39 (a) N. Henry, O. Mentre, F. Abraham, E. J. MacLean, P. Roussel *J. Solid State Chem.*, 2006, **179**, 3087-3094; (b) N. Henry, M. Evain, Ph. Deniard, S. Jobic, F. Abraham, O. Men tre *Z. Naturforsch. B* 2005, **60**, 322-327.

40 (a) S.-C. Wang and N. Ye, *J. Am. Chem. Soc.*, 2011, **133**, 11458-11461; (b) G. X. Wang, M. Luo, N. Ye, C. S. Lin and W. D. Cheng, *Inorg. Chem.*, 2014, **53**, 5222-5228; (c) S. C. Wang, N. Ye, W. Li and D. Zhao, *J. Am. Chem. Soc.*, 2010, **132**, 8779-8786.

41 H. A. Reshak, X. Chen, S. Auluck and H. Kamarudin, *Mater. Res. Bull.* 2012, **47**, 2552–2560.

